Accepted Manuscript

Research papers

Tracer sampling frequency influences estimates of young water fraction and streamwater transit time distribution

Michael P. Stockinger, Heye R. Bogena, Andreas Lücke, Bernd Diekkrüger, Thomas Cornelissen, Harry Vereecken

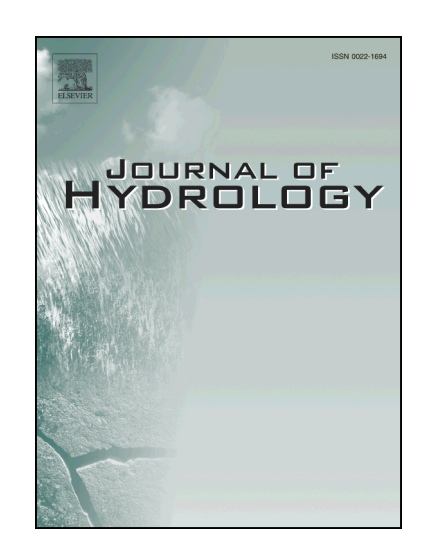
PII: S0022-1694(16)30486-3

DOI: http://dx.doi.org/10.1016/j.jhydrol.2016.08.007

Reference: HYDROL 21442

To appear in: *Journal of Hydrology*

Received Date: 17 June 2016
Revised Date: 2 August 2016
Accepted Date: 3 August 2016



Please cite this article as: Stockinger, M.P., Bogena, H.R., Lücke, A., Diekkrüger, B., Cornelissen, T., Vereecken, H., Tracer sampling frequency influences estimates of young water fraction and streamwater transit time distribution, *Journal of Hydrology* (2016), doi: http://dx.doi.org/10.1016/j.jhydrol.2016.08.007

This is a PDF file of an unedited manuscript that has been accepted for publication. As a service to our customers we are providing this early version of the manuscript. The manuscript will undergo copyediting, typesetting, and review of the resulting proof before it is published in its final form. Please note that during the production process errors may be discovered which could affect the content, and all legal disclaimers that apply to the journal pertain.

Tracer sampling frequency influences estimates of young water fraction and streamwater transit time distribution

Michael P. Stockinger*, Heye R. Bogena, Andreas Lücke, Bernd Diekkrüger, Thomas Cornelissen, Harry Vereecken

Authors' addresses:

Michael P. Stockinger, Andreas Lücke, Heye R. Bogena and Harry Vereecken

Forschungszentrum Jülich GmbH, Institute of Bio- and Geosciences, Agrosphere Institute (IBG-3), Wilhelm-Johnen-Straße, 52425 Jülich, Germany

Bernd Diekkrüger and Thomas Cornelissen

Bonn University, Department of Geography, Meckenheimer Allee 166, 53115 Bonn, Germany

*Corresponding author: Michael Paul Stockinger, Forschungszentrum Jülich GmbH, Agrosphere Institute (IBG-3), Wilhelm-Johnen-Straße, D-52425, Germany, Tel +49 2461 61 5484, m.stockinger@fz-juelich.de

ABSTRACT

The streamwater transit time distribution (TTD) of a catchment is used to derive insights into the movement of precipitation water via various flow paths to the catchment's stream. Typically, TTDs are estimated by using the convolution integral to model a weekly tracer signal measured in streamflow. Another approach for evaluating the transit time of water to the catchment stream is the fraction of young water (F_{yw}) in streamflow that is younger than a certain threshold age, which also relies on tracer data. However, few studies used tracer data with a higher sampling frequency than weekly. To investigate the influence of the sampling frequency of tracer data on estimates of TTD and F_{yw} , we estimated both indicators for a humid, mesoscale catchment in Germany using tracer data of weekly and higher sampling frequency. We made use of a 1.5 year long time series of daily to sub-daily precipitation and streamwater isotope measurements, which were aggregated to create the weekly resolution data set. We found that a higher sampling frequency improved the stream isotope simulation compared to a weekly one (0.35 vs. 0.24 Nash-Sutcliffe Efficiency) and showed more pronounced short-term dynamics in the simulation result. The TTD based on the high temporal resolution data was considerably different from the weekly one with a shift towards faster transit times, while its corresponding mean transit time of water particles was approximately reduced by half (from 9.5 to 5 years). Similar to this, F_{vw} almost doubled when applying high resolution data compared to weekly one. Thus, the different approaches yield similar results and strongly support each other. This indicates that weekly isotope tracer data lack information about faster water transport mechanisms in the catchment. Thus, we conclude that a higher than weekly sampling frequency should be preferred when investigating a catchment's water transport characteristics. When comparing TTDs or F_{yw} of different catchments, the temporal resolution of the used datasets needs to be considered.

KEYWORDS

Catchment hydrology

ACCEPIED MANUSCRIP

1 Introduction

Many studies of catchment transit time distributions (TTDs), representing the different flow paths taken by precipitation water during catchment passage, and of the mean transit time (MTT), the average time a water parcels needs to exit the catchment after entering it as precipitation, used weekly sampling intervals for chemical [Hrachowitz et al., 2009; Molenat et al., 2013] or isotopic tracer data [Rodgers et al., 2005; Stockinger et al., 2014; Tetzlaff et al., 2007; Viville et al., 2006]. Only few studies applied data with a higher sampling frequency [Kirchner et al., 2000; Roa-Garcia and Weiler, 2010]. For example, using a sub-daily sampling frequency for several events, Roa-Garcia and Weiler [2010] found evidence of time-variable MTTs when looking at event and base flow conditions. Birkel et al. [2012] refined this knowledge by estimating TTDs of a one year long time series using daily precipitation and weekly, daily and 4h (during two events) streamflow stable isotope data $(\delta^8 O)$ and δH), respectively. They found evidence for time-variable TTDs with summer and winter runoff events differing in MTTs. Consequently, Birkel et al. [2012] argue for the value of high-frequency sampling to evaluate the feasibility of MTTs derived with data sets of e.g., weekly sampling intervals. This argument is supported by findings of Berman et al. [2009], who found fine-scale changes in the isotopic composition of precipitation measuring up to 90 samples per day. Additionally, the need for high-resolution tracer data to move forward in the hydrological sciences was recently emphasized [McDonnell and Beven, 2014], while Kirchner et al. [2004] pointed out the importance of high-frequency chemical data for a better understanding of catchment hydrology.

The effect of sampling frequency of tracer data on estimates of MTTs was investigated by *Hrachowitz et al.* [2011]. They used weekly precipitation and stream isotope data to estimate MTTs of a Scottish catchment and found increasing errors in MTTs while increasing the

sampling interval up to 8 weeks. They argue that internal catchment processes will be misrepresented when using a reduced sampling frequency.

More recently, the study of *Timbe et al.* [2015] of a tropical montane cloud forest catchment compared different sampling frequencies of stable isotope data ranging from daily to bimonthly and found that it affected estimates of TTDs for soil and stream water. However, in their study the case of daily sampling intervals was based on daily precipitation data only, while the stream was sampled weekly. Additionally, modeling focused on baseflow conditions, as samples of several rainfall-runoff events were discarded, potentially missing faster flow conditions in their analysis.

The effect of using long-term isotope tracer data of streamwater and precipitation with a daily or sub-daily sampling frequency on estimated TTDs and MTTs has not yet been studied. Considering the argument of *Hrachowitz et al.* [2011] that high-resolution data can potentially better represent internal catchment processes, the hydrological community faces the risk of acquiring a biased understanding of catchment runoff generation processes when using low temporal resolution data. Furthermore, the comparison of TTDs of different catchments derived from data sets with different sampling frequencies may lead to ambiguous results (e.g., the study of *Heidbüchel et al.* [2012] using fortnightly isotope tracer data for one catchment, while using daily isotope tracer data for a different catchment).

Many of the prior studies used the convolution integral approach to derive the TTD and MTT from tracer data. Recently, *Kirchner* [2016a] and *Kirchner* [2016b] tested a similar approach by fitting sine waves to the tracer signal of precipitation and streamflow and derived the MTT using the change in amplitude and the occurring phase shift. Both studies show that the sine wave method is not able to derive correct MTTs under the condition of spatial heterogeneity [*Kirchner*, 2016a] and non-stationarity [*Kirchner*, 2016b]. As every catchment is heterogeneous and non-stationary to some degree, the sine wave fitting method is not suitable

to derive TTDs and MTTs. Accordingly, a new measure was proposed which could be correctly estimated, which is the fraction of young water, F_{yw} [Kirchner, 2016a]. F_{yw} represents the fraction of water that is younger than a certain threshold age. It remains a topic of future studies to test whether the convolution integral suffers from equal aggregation bias errors as the sine wave method.

In this study, we investigated the hypotheses that (1) a higher sampling frequency improves the quality of stable isotope modeling of streamwater in terms of an objective function metric, and (2) the TTD is a function of sampling frequency. To this end, we estimated TTDs using the convolution integral approach. As *Kirchner* [2016a] showed the potential of aggregation bias error when using the convolution integral, which would result in a highly uncertain understanding of the impact of sampling frequency on a catchment's water transport characteristics, we additionally investigated an independent proof-of-concept metric with the hypothesis that (3) F_{yw} is a function of sampling frequency.

The data for this study consisted of stable isotope data (δ^8O) with a temporal resolution of 0.5 day for precipitation and daily and 4h for streamflow under baseflow and event conditions, which were mathematically aggregated to a weekly temporal resolution.

2 Methods

2.1 Study Site

The Erkensruhr catchment (41.7 km²) is located in the western part of Germany at an altitude between 286 m asl. in the northern to 631 m asl. in the southern part (Figure 1). The catchment's climate is humid with a distinct precipitation gradient (annual precipitation increases from 740 mm in the eastern part to 1150 mm in the western part). The mean annual temperature ranges from 7.6 °C for higher to 10.0 °C for lower altitudes. The catchment is part of the national park Eifel and dominantly covered by coniferous forest in the south and

deciduous forest and grassland in the north (Figure 1, Table 1). Soils in the catchment primarily are cambisols with the exception of river valleys where gleysols and planosols can be found. The base rock is Devonian clay shale with sandstone intrusions [*Stoltidis and Krapp*, 1980].

2.2 Measured Data

We used hydrological and isotopic data to estimate TTDs and F_{yw} for the time period of 3rd October 2012 to 8th March 2014. Additionally, data from 24th November 2010 to 2nd October 2012 was used to spin up the model that was applied to estimate TTDs (Figure 2, Figure S1 in Supplemental Material).

Precipitation amount data (1 hour resolution, 0.1 mm increment) was acquired from the Schöneseiffen meteorological station (620 m asl.) located at the southeastern border of the catchment (Figure 1). To account for the catchment's precipitation gradient we used precipitation radar data from the Neuheilenbach station (585 m asl., German Weather Service, DWD). Radar pixel sizes varied between 0.95 and 2.1 km² and precipitation was determined in five minute intervals. A global rescaling factor was applied to the precipitation amounts of each pixel so that the value of the pixel to which the Schöneseiffen station belongs equals '1'. We then calculated the arithmetic mean of the pixel values within the Erkensruhr catchment to represent the catchment's average areal precipitation amounts in comparison to Schöneseiffen. Finally, the Schöneseiffen precipitation time series was multiplied with this value to rescale it to the Erkensruhr precipitation input. Additionally, snow data acquired from the meteorological station Kalterherberg (German Weather Service, station number 80115, 535 m asl.) located approximately 9 km to the west of the Erkensruhr catchment was used to account for snow blanket buildup in hydrological modeling.

Stream stage data (15 minute resolution, 1 mm increment) is available from 2001 to the present (courtesy of the local water board, Wasserverband Eifel-Rur) and was converted to runoff using a polynomial regression to the 4th power (R² = 0.99, not shown). Situated in the south of the Erkensruhr catchment lies the well-studied Wüstebach sub-catchment which is one of the Terrestrial Environmental Observatories (TERENO) test sites [*Bogena et al.*, 2015; *Zacharias et al.*, 2011]. Soil water content (SWC) data from this location was used to aid in estimating TTDs of the Erkensruhr.

As about 55% of the catchment is forest-covered and canopy interception influences the estimates of TTDs [Stockinger et al., 2015], different kinds of precipitation δ^8 O samples were taken at three different locations throughout the catchment: (1) throughfall (TF) samples of a deciduous forest (Im Brand, IB) in weekly resolution; (2) TF samples of a coniferous forest (Wüstebach, WU) in weekly resolution; and (3) open land (OP) samples at the Schöneseiffen meteorological station in 0.5 day resolution. We could not sample the location Im Brand from δ^{th} November 2012 to 17^{th} May 2013 due to administrative issues. While TF was sampled using RS200 samplers that were already successfully applied in the precipitation isotope study of Stockinger et al. [2015], OP was sampled by a cooled, automated sampler (NSA 181/KS-16, Eigenbrodt).

To create a single high resolution precipitation δ^8 O time series necessary for modeling, we first amount-weighted the high resolution OP isotope data according to the sampling dates of the TF samples to create weekly OP isotope data. Then we calculated the weekly isotopic differences of the weighted OP data to measured TF at the forest stations WU and IB, respectively. This was done in such a way that a positive difference indicates enrichment in isotope values of TF when compared to OP, as can often be observed [*Dewalle and Swistock*, 1994]. To create the high resolution TF data for both forest locations, these weekly differences were added to the high resolution OP values of the respective weeks. Finally, the

three high resolution time series of OP, IB and WU were unified into a single high resolution time series by weighing them according to the Erkensruhr land use percentages (see Table 1) of coniferous forest (WU), deciduous forest (IB) and the remaining land uses (OP).

The amount-weighted, weekly OP was further used to verify OP isotope measurements at Schöneseiffen against (a) data of weekly bulk samples from an independent cooled sampler at Schöneseiffen, (b) TF from the location IB in the north of the catchment to investigate a possible intra-catchment gradient in precipitation isotopes, and (c) TF from the location WU.

Stream samples for stable isotope analysis were taken in daily time steps during low flow conditions and 4h time steps during high flow conditions using a cooled, automated sampler (Liquistation CSF48, Endress+Hauser). The threshold for switching between low and high flow conditions was adjusted at irregular intervals and subjectively chosen according to the respective water level to guarantee isotopic characterization of several runoff events. The sampler stream isotope data was verified against manually taken weekly grab samples from the same location.

As only the stream stage data was available for the spin up phase, the other necessary data was acquired from different sources as the ones used for the modeling phase. Precipitation amounts were acquired from the Kalterherberg station (1 hour resolution, 0.1 mm increment, DWD) and correlated to Schöneseiffen precipitation amounts. We then calculated the spin up precipitation amounts by multiplying the Kalterherberg data with the obtained regression slope value and the rescaling factor obtained by the precipitation radar procedure. We used precipitation δ^8 O from the weekly, cooled bulk samples taken at Schöneseiffen. For stream δ^8 O we correlated the available Erkensruhr δ^8 O time series to the Wüstebach sub-catchment's which extends to the necessary time period. The resulting regression equation with an R^2 =

0.45 was deemed suitable for the purpose of spinning up the model and thus used to create weekly Erkensruhr stream isotope data.

Due to the high correlation of Wüstebach and Erkensruhr runoff values (R² = 0.88, not shown) and the lack of catchment-wide SWC information for the Erkensruhr catchment, we used data of a wireless SWC measurement network (SoilNet) installed in the Wüstebach sub-catchment to estimate changes in hydrological response behavior of the Erkensruhr catchment (for details on SoilNet refer to *Bogena et al.* [2010] and *Rosenbaum et al.* [2012]). We do not assume that the Wüstebach soil water content values were quantitatively valid for the whole Erkensruhr catchment, but rather that the trend of SWC in the Wüstebach was qualitatively sufficient to estimate the changes in hydrological behavior of the Erkensruhr catchment.

Water isotopic analysis was carried out using two measurement systems: (1) an Isotope-Ratio Mass Spectrometer (Delta V Advantage, Thermo Scientific) coupled with a high temperature pyrolysis furnace (HT-O, HEKAtech), and (2) laser-based cavity ringdown spectrometers (models L2120-i and L2130-i, Picarro). Results are reported as δ values relative to Vienna Standard Mean Ocean Water (VSMOW) [Brand et al., 2014], where $\delta = (R_S/R_{St}$ -1)*1000 with R_S and R_{St} as isotope ratios ($^{18}\text{O}/^{16}\text{O}$) of samples and standards, respectively. Internal standards calibrated against VSMOW, Standard Light Antarctic Precipitation (SLAP2) and Greenland Ice Sheet Precipitation (GISP) were used to calibrate raw data and to ensure long-term stability of analyses. The integrity of measurement results between the mass spectrometer and the laser-based systems was verified within the measurement uncertainties by measuring reference waters with all systems. The precision of the analytical systems was \leq 0.1 %e for $\delta^8\text{O}$.

2.3 TTD Calculation

TTDs were estimated in hourly time steps with the conceptual model TRANSEP [Weiler et al., 2003]. First, effective precipitation (p_{eff}), the fraction of total precipitation that is not lost to evapotranspiration and deep percolation, is estimated by modeling the observed hydrograph:

$$Q(t) = \int_0^t g(\tau_R) p_{eff}(t - \tau_R) d\tau_R \tag{1}$$

where Q(t) is the simulated runoff at time t, $g(\tau)$ is the Response Time Distribution (RTD), τ the response time and $p_{eff}(t-\tau)$ is the effective precipitation for time step $t-\tau$. While the TTD describes the actual water particle transport through the catchment, the RTD also includes hydraulic pressure waves propagating through the soil [Rinaldo et al., 2011]. Estimation of p_{eff} was done using a non-linear Antecedent Precipitation Index (API) approach [Jakeman and Hornberger, 1993]:

$$p_{eff} = p(t)s(t) \tag{2a}$$

$$s(t) = b_1 p(t) + (1 - b_2^{-1}) s(t - \Delta t)$$
(2b)

where p(t) is precipitation, s(t) the API, Δ the calculation time step of 1 h, b_1 a scaling factor to match the amount of total simulated runoff to the amount of total p_{eff} and b_2 is weighing each precipitation event backward in time. An additional parameter, b_3 , sets the initial API conditions for time step t = 0.

Modeling of the hydrograph with Equation 1 included a simple snow model [Stockinger et al., 2014] to account for the time delay in precipitation water input to the catchment in case of buildup of a snow blanket. We used the snow data acquired from the Kalterherberg meteorological station to identify times of snow blanket build up. During those times, all precipitation was conceptually stored in a reservoir. In case of partial or full melt, a volume-

proportional amount of melt water was released from this conceptual reservoir over the course of six hours.

Similar to the method used in *Stockinger et al.* [2014] for the Wüstebach sub-catchment, the hydrograph of the Erkensruhr was split into individual modeling periods to estimate p_{eff} by using SWC measurements of the Wüstebach. This was done as the modeling result using the complete hydrograph resulted in over-predictions during summer months, while winter months were under-predicted (not shown). The modeling periods used in this study describe the catchment's wet and dry states in terms of overall catchment wetness. For each modeling period we assumed quasi-constant hydrological behavior. In terms of the RTD, this means a constant RTD for each individual modeling period. Thus the hydrograph was split into three distinct modeling periods: a wet state followed by a dry state and a wet state again. They will from now on be referred to as 'Winter_12', 'Summer_13' and 'Winter_13' (Figure 2). As the model is re-initialized with 0 mm/h runoff at the beginning of each modeling period, we omitted plotting the unavoidable artefacts of very small runoff values at the beginning of each phase.

During early modeling it became apparent that the described approach applied at the Wüstebach (0.385 km²) was not sufficient for the hundredfold larger Erkensruhr (41.7 km²). Peak runoff situations were not modeled adequately (not shown) which could pose a problem with the high resolution isotope stream data that captured many peak runoff situations. Thus, to better simulate these situations and to better characterize the catchment's response to precipitation, several steps had to be taken.

First, we identified extreme runoff situations (i.e., events) during the wet and dry states and modeled them individually. For the wet states, we defined the start of an event as the exceedance of the 97.5% confidence band of the daily hydrograph gradient. Events ended when the falling hydrograph limb either a) reached the 5%-quantile of runoff values of the

respective wet state or, b) was intercepted by another event (Figure 4). We then estimated p_{eff} individually for these wet state events by subtraction of the base flow, which was identified as the lowest observed runoff value during the event. To compare the response of the catchment, we combined the RTDs of the non-event and the event modeling periods by weighting them according to their temporal proportion of the hydrograph. Contrary to this, dry state events had a much shorter duration and it was necessary to use the hourly hydrograph gradient instead of the daily one to identify events. We estimated p_{eff} for dominant events by first subtracting the mean runoff of the three days prior an event from the runoff of the first two event hours. The ratio of the resulting value to the peak runoff was multiplied with the event precipitation amount to estimate p_{eff} (also see *Stockinger et al.* [2014] and the event of 3rd July 2010 mentioned in their study). This assumes that within two hours the fast response of the catchment to an extreme rainfall event has finished and the rest of the event runoff stems from past precipitation water.

Second, even with the event-separated p_{eff} estimation the modeling of the dry state (Summer 2013) resulted in a non-realistic hydrograph simulation (Figure 3). Thus, this modeling period was further separated into a main phase that is preceded by a drying phase and followed by a wetting-up phase. A large part of the dry state (from now on referred to as the main phase) could be characterized by a linear trend fitting a major part of the log-transformed hydrograph. However, this linear trend did not describe the whole modeling period but only the central part. Thus, the beginning and end of the dry state were interpreted as a drying ('D' in Figure 3) and a wetting-up ('W' in Figure 3) phase separated in their hydrological characteristic from the main phase. The p_{eff} of these three phases of the dry state were thus also modeled individually.

After p_{eff} estimation, the TTD was estimated by modeling the isotope tracer signal in the stream:

$$C(t) = \frac{\int_0^t C_{in}(t-\tau_T)p_{eff}(t-\tau_T)h(\tau_T)d\tau_T}{\int_0^t p_{eff}(t-\tau_T)h(\tau_T)d\tau_T}$$
(3)

where C(t) is the simulated streamwater isotope concentration at time t, $p_{eff}(t - \tau)$ is effective precipitation for time $t - \tau$, $C_{in}(t - \tau)$ is the precipitation isotope concentration at time $t - \tau$ with transit time τ and $h(\tau)$ is the TTD, which is calibrated during the modeling of the isotope tracer signal in the stream.

We used the two-parallel linear reservoirs model for the RTDs and TTDs, as it showed good results in previous studies (e.g., *Stockinger et al.* [2015]):

$$g(\tau_R) = \frac{\phi}{\tau_f} \exp\left(-\frac{\tau_R}{\tau_f}\right) + \frac{1-\phi}{\tau_s} \exp\left(-\frac{\tau_R}{\tau_s}\right)$$
 (4)

$$h(\tau_T) = \frac{\phi}{\tau_f} \exp\left(-\frac{\tau_T}{\tau_f}\right) + \frac{1-\phi}{\tau_s} \exp\left(-\frac{\tau_T}{\tau_s}\right)$$
 (5)

where ϕ is a partitioning factor (between 0 and 1) and τ and τ are the mean transit times of the fast and slow reservoirs, respectively.

The corresponding mean response time (MRT) and MTT were calculated from the twoparallel linear reservoirs parameters:

$$MRT \text{ or } MTT = \tau_f * \phi + \tau_s * (1 - \phi)$$
 (6)

To objectively evaluate the hydrograph simulation we used the Volumetric Efficiency (VE) as it equally evaluates low and high flow conditions. To emphasize an adequate modeling of isotopic peaks considering the high resolution isotope tracer data, we used the Nash-Sutcliffe Efficiency (NSE) for the stream isotope simulation, as the NSE is sensitive to time series peaks [*Criss and Winston*, 2008; *Nash and Sutcliffe*, 1970]:

$$VE = 1 - \frac{\sum |Q_{sim} - Q_{obs}|}{\sum Q_{obs}} \tag{7}$$

$$NSE = 1 - \frac{\sum (C_{obs} - C_{sim})^2}{\sum (C_{obs} - \overline{C_{obs}})^2}$$
 (8)

where Q_{obs} , Q_{sim} , C_{obs} and C_{sim} are observed and simulated runoff and streamwater isotope concentration respectively.

The parameter space was searched using the Ant Colony Optimization algorithm [Abbaspour et al., 2001].

2.4 Fraction of young water

We calculated the fraction of young water F_{yw} for each temporal resolution following *Kirchner* [2016a]: First, sine waves were fitted to the precipitation and the streamflow isotope time series, respectively. To do this, we determined the cosine and sine coefficients a_P and b_P (precipitation) and a_S and b_S (streamflow) of the multiple linear regression functions:

$$C_P(t) = a_P \cos(2\pi f t) + b_P \sin(2\pi f t) + k_P,$$

$$C_S(t) = a_S \cos(2\pi f t) + b_S \sin(2\pi f t) + k_S \tag{9}$$

with $C_P(t)$ and $C_S(t)$ being the tracer signal in precipitation and streamflow at time t, f the frequency of the fitted sine wave, and k_P and k_S represent the vertical shift of the sine wave. Due to the annual seasonal behavior of precipitation and streamflow isotopes, the frequency of this study was set to 1/8766 hours (365.25 x 24, i.e., 1 per year).

Fitting was done by using the iteratively reweighted least squares method, which limits the influence of outliers. Precipitation isotope values were weighed by their respective bulk precipitation amounts, while streamflow isotope values were weighed by the runoff value at the time of streamflow sampling.

The amplitudes A_P and A_S and the phase shift of each sine wave φ and φ was calculated by:

$$A_P = \sqrt{a_P^2 + b_P^2}, \qquad A_S = \sqrt{a_S^2 + b_S^2},$$

$$\varphi P = \tan -1(aPbP), \quad \varphi = \tan -1(aSbS)$$
 (10)

Contrary to the calculation method in *Kirchner* [2016a], the phase shift between precipitation and streamflow sine waves $\varphi - \varphi$ was derived by the arctangent of the vector cross product over the vector dot product of precipitation and streamflow coefficients, as this is a better way of finding the phase shift than the simple subtraction (personal communication *Kirchner*, May 2016):

$$\mathscr{O} - \mathscr{P} = \tan -1(aPbS - aSbP)/(aPaS + bPbS)$$
(11)

With the amplitude ratio A_S/A_P and the phase shift $\varphi - \varphi$ we then calculated the shape parameter α of the gamma distribution function $\Gamma(\varphi)$ that represents the catchment's TTD by iteratively solving:

$$\mathscr{G} - \mathscr{P} = \alpha \tan -1((AS/AP) - 2/\alpha - 1) \tag{12}$$

The scale parameter β of $\Gamma(\alpha\beta)$ was calculated with:

$$\beta = \frac{1}{2\pi f} \sqrt{(\frac{A_S}{A_P})^{-2/\alpha} - 1}$$
 (13)

Using α we then found the threshold age τ_w for the fraction of water younger than this age, F_{yw} , by using the regression equation of *Kirchner* [2016a]:

$$\tau_{yw} = 0.0949 + 0.1065\alpha - 0.0126\alpha^2 \tag{14}$$

As the final step, F_{yw} was calculated with the lower incomplete gamma function $\Gamma(\tau_{yw}, \alpha\beta)$:

$$F_{yw} = \Gamma(\tau_{yw}, \alpha, \beta) = \int_{\tau=0}^{\tau_{yw}} \frac{\tau^{\alpha-1}}{\beta^{\alpha} \Gamma(\alpha)} e^{-\frac{\tau}{\beta}} d\tau$$
 (15)

Calculation of F_{yw} was carried out once as described and for comparison once with the much simpler approach also described in *Kirchner* [2016a], in which F_{yw} equals the amplitude ratio A_S/A_P .

2.5 Uncertainty estimation

The individual uncertainties of the convolution integral method and of F_{yw} were derived as follows: for the convolution integral the parameter uncertainties were obtained by first identifying the 95%-confidence limits of the posterior parameter distribution of the last third of parameter sets that were used by the Ant Colony Optimization search algorithm. These limits were then used as parameter boundaries for 1000 Monte Carlo simulations (MATLAB toolbox "MCAT v.3). The minimum and maximum stream isotope and TTD values found by all 1000 Monte Carlo runs were defined as the uncertainty limits. The observed stream isotope uncertainty corresponds to the measurement precision.

For the fraction of young water we defined a tight and a wider uncertainty: the tight uncertainty of F_{yw} was defined on one hand by the result of the simple calculation method of deriving F_{yw} (only using A_S/A_P) and on the other hand by the result of the more complex approach (additionally using $\varphi - \varphi$). The wider uncertainty was found during calculation, as some of the parameters of the multiple linear regressions used in Equation 9 showed large p-statistic significance values (far larger than the usually applied 0.05 limit). We thus propagated the errors to the results by once adding and second subtracting the error estimate of the estimated coefficients with the large p-statistics. From all the resulting combinations, we chose the minimum and maximum values of the results to define the wider uncertainty for F_{vw} .

3 Results and Discussion

8 O of the weekly amount-weighted OP was highly correlated with the weekly Schöneseiffen bulk samples and TF isotopes measured at IB and WU ($R^2 = 0.88$ with slope 1.02 for the bulk samples, and $R^2 = 0.77$ with slope 1.06 and $R^2 = 0.86$ with slope 1.08 for IB and WU, respectively). Stream isotope data was verified against the weekly grab samples ($R^2 = 0.69$, Figure 2c). A direct comparison of OP and TF for the purpose of identifying an isotopic precipitation gradient is complicated because, in comparison to OP, TF is reduced in precipitation amount and its stable isotope values are affected by canopy passage. However, precipitation input to the Erkensruhr catchment did at least not show a strong isotopic gradient based on cardinal directions or altitude. The similarities of TF and OP only support the assumption of homogeneous above-canopy precipitation isotopes. Canopy-induced changes in TF isotope values compared to OP might seem negligible, but are actually important for TTD estimation and hydrograph separation [Kubota and Tsuboyama, 2013; Stockinger et al., 2015]. To account for the effect of TF on estimates of streamwater TTD, we used a land-use based weighing of three point-measurements, two of which were TF with a weekly resolution only. With this approach we inherently assumed each point-measurement to be representative for the land-use unit it was situated in. However, several studies showed the influence of canopy structure on the isotopic composition of TF [Brodersen et al., 2000; Kato et al., 2013] and problems of TF sampling systems with small precipitation amounts [Zimmermann and Zimmermann, 2012]. It is not likely that the Erkensruhr coniferous and deciduous forests are uniform in canopy structure throughout the catchment. Nonetheless, we assumed the uncertainties associated with this land-use based weighting approach to be negligible in comparison to the effect of different tracer data resolutions and based this assumption on the good correlations between OP and TF isotope measurements throughout the catchment.

The precipitation radar data showed that the distributed precipitation amounts over the Erkensruhr catchment amounted on average to 92% of the recorded Schöneseiffen amounts (94% for 2010, 90% for 2011). Thus, Schöneseiffen precipitation amounts were multiplied with a global rescaling factor of 0.92. This simple method to account for the precipitation gradient of the catchment was assumed to be sufficient for use with the simple conceptual model applied in this study, which assumes a uniform spatial distribution of rainfall. Erkensruhr runoff was highly correlated with runoff and SWC measured at Wüstebach (R^2 = 0.88 and 0.89, respectively). Uniformity in at least temporal occurrence of precipitation is confirmed by the high correlation of the Wüstebach and Erkensruhr runoff. Stockinger et al. [2014] have shown that a strong relationship between overall catchment wetness of the Wüstebach and its hydrological response behavior exists. Similar to *Graf et al.* [2014], they expressed the overall catchment wetness as the average of the spatiotemporal high resolution SWC. The high correlation of the Erkensruhr runoff to the Wüstebach's runoff and SWC indicates that the Wüstebach SWC can be used as an appropriate indicator of the catchment wetness of the Erkensruhr catchment. Thus, we can assume that the switching from wet to dry states found in the Wüstebach catchment [Stockinger et al., 2014] also takes place in the whole Erkensruhr catchment. A possible mechanism driving this is the balance between water and energy input to both catchments [Heidbüchel et al., 2012]. Our assumption is supported by the successful splitting of the hydrograph into modeling periods of mostly uniform hydrologic behavior (except for event runoff situations), and the subsequent satisfying simulation of the Erkensruhr hydrograph (see below). This highlights the importance of measuring SWC data [Vereecken et al., 2008] and shows that the method for splitting the hydrograph into periods of quasi-constant hydrological behavior applied by Stockinger et al. [2014] can be transferred to higher-order catchments at least.

The usage of the simple snow model of *Stockinger et al.* [2014] may have led to additional uncertainties in the hydrograph simulation, e.g., compaction of the snow blanket is not accounted for. However, snow only sparsely occurred during the modeling period. Furthermore, the hydrograph modeling results slightly improved (from VE = 0.62 to VE = 0.66) while peak height and timing could be better simulated (not shown). Thus, we believe the shortcomings of this simple snow model in relation to our overall not too complex modeling setup to be negligible.

3.1 Stable isotope modeling of streamwater

Hydrograph simulation results for all modeling periods showed overall good VE values ranging from 0.59 to 0.83 (Figure 5a, Figure 6 and Table 2) with a total p_{eff} of 780 mm. Although several runoff events were well modeled, some runoff peaks were underestimated. The MRTs increased from the event phase of Winter_12 to the non-events (Winter_12 and Winter_13) and to Summer_13 (Figure 7, Table 2). Combining both the non-event and the event simulation of Winter_12 resulted in a RTD that matched the one of Winter_13 (Winter_12 (C) compared to Winter_13 in Figure 7). A similar catchment response during wet states was already observed in *Stockinger et al.* [2014], where the Wüstebach catchment also showed matching RTDs. Furthermore, the Wüstebach's two dry states responded similarly too. This could however not be compared to the present study, as the modeling period of the Erkensruhr only comprises one dry state. A seasonal cycle of a catchment's hydrologic response was also found for the humid Rietholzbach catchment in the study of *Heidbüchel et al.* [2012] by using a time-varying TTD approach rather than splitting up the hydrograph.

The delineation of runoff events during the wet states resulted in five identified events (Figure 4). The four events of Winter_12 surpassed the 97.5% daily hydrograph gradient at the beginning of the rising hydrograph limb. They directly followed each other and thus were

modeled as one segment, meaning one RTD was used for all four events. For the single event of Winter_13 the 97.5% threshold was exceeded at the peak of the rising hydrograph. Due to this, it was not modeled separately and no p_{eff} values were updated. For Summer_13, the dry state, we used the hourly hydrograph gradient and identified three dominant events where p_{eff} was modeled separately. Comparison of average runoff before those events and peak runoff in the first two hours resulted on average in 95% of event rainfall becoming p_{eff} and creating a quick response in stage level at the outlet within two hours (Figure 4).

The drying and wetting-up phase of Summer_13 had similar MRTs which were in between the longer MRT of Summer_13 and the shorter MRTs of both winters (Table 2). Similar to this, Birkel et al. [2012] found longer transit times for events with low antecedent wetness (in the terms of this study: the dry state). Heidbüchel et al. [2012] explained this by differences in storage as well as precipitation and energy input to the catchment. This finding is in contrast to the behavior of the Wüstebach sub-catchment reported in Stockinger et al. [2014], which had shorter response times during dry conditions. The authors argued that the Wüstebach's hillslopes disconnect hydrologically from the runoff-generation process during the dry state, thus disconnecting primarily slow flow paths. This assumption may be valid for a small headwater catchment with shallow soil depths, but a complete disconnection of all slow flow paths during dry states becomes less likely with increasing catchment size due to more varied land-use, topography, soil depths, etc., creating buffering and superposition effects in the hydrograph. As the Erkensruhr's geology changes in the Northern part, the detection of a complete or partial disconnection of slow flow paths during dry states could be impaired and is subject of future research. Despite the contrasting seasonal response behavior, the runoff of Erkensruhr and Wüstebach was highly correlated ($R^2 = 0.88$), which can be attributed to the generally shallow soil depths, extremely low conductivity of the bedrock in the Erkensruhr catchment and the uniform spatial occurrence of precipitation input. We argue that these

relatively short flow paths (limited by the shallow soil depth) led to a similar response of both hydrographs on the hourly time scale. Contrary to this, the RTD captures the overall reaction of the catchment during the complete modeling period, far exceeding the hourly time step.

The stream isotope simulation was better optimized when using high resolution data compared to using weekly data (NSE = 0.34 vs. NSE = 0.24, respectively). This comparison is based on calculating the high resolution NSE solely for isotope values that were also observed in the weekly resolution case (Table 3). Considering all observed values of the high resolution case resulted in an NSE value of 0.22, which is slightly lower than the one of the weekly resolution case. Winter_13 was not well modeled in terms of stream isotopes, with the simulation result overpredicting for both the weekly and the high resolution case. While results based on high resolution data had an NSE of 0.34 when considering the modeling periods before Winter_13, it became -2.01 for Winter_13. The unsatisfying modeling result of Winter_13 could be explained with the simplified model assumptions of TRANSEP, e.g., a time-invariant TTD. Using a model based on time-variant transit times, e.g., that of *Klaus et al.* [2015], may improve the simulation results. Generally, both the weekly and high resolution tracer data had comparatively low NSE values that were however comparable to results of the Wüstebach sub-catchment's outlet found in *Stockinger et al.* [2014].

Comparison of the simulated stream isotopes revealed that the high resolution case was able to reproduce short term dynamics with sudden steep changes in isotope values, e.g., at the beginning of 2013 or at the beginning of Winter_13. Comparing this to the weekly resolution results, the beginning of 2013 did not show such a steep increase in stable isotope values, while the decrease in values in Winter_13 is completely missing (Figure 5c).

3.2 The TTD estimated by the convolution integral

There is a tradeoff between capturing long-term dynamics and short-term peaks of the streamwater isotope signal concurrently, which is reflected in the isotope simulation results and estimated TTDs (Figure 8). While the high resolution simulation features more short-term dynamics, both data resolutions nonetheless focused on capturing the long-term behavior of the isotope time series (Figure 5c). This is reflected in the respective TTDs, where the high resolution TTD emphasized faster flow paths in contrast to the weekly TTD. Because of this, the high resolution data allows for simulation of short-term peaks, e.g., the second isotope peak at the beginning of the time series, or the short-term decrease of isotope values in November 2013, all of which are absent in the rather smooth weekly simulation result. However, the long tails of both TTDs are similar in form, reflecting the emphasis of both simulations to capture the long-term behavior of the streamwater isotope time series. This explains the overall similarities of the isotope simulations of high resolution and weekly data, despite vastly differing TTDs.

Overall, transit times based on weekly resolution were longer than the ones based on high resolution data, with MTTs of 9.53 and 4.66 years, respectively (Figure 8, Table 3). This finding is corroborated by *Hrachowitz et al.* [2011], who used weekly data and found that MTT absolute errors increase with increasing sampling intervals. Contrary to this, in *Timbe et al.* [2015] the MTTs of the weekly and daily case are almost indistinguishable. This discrepancy might be related to the use of weekly streamwater isotope data in *Timbe et al.* [2015], while this study used at least daily (and several times 4-hourly) data. At the same time the data resolution of precipitation is higher compared to the former study (0.5 day versus 1 day) which might also have had an impact on the magnitude of differences in MTTs of weekly and higher data resolutions.

The application of stable isotopes with the convolution integral reaches its limit for MTTs longer than 4-5 years, as longer MTTs often lead to isotope signal variations in the stream that

are smaller than the measurement error, thus becoming effectively invisible to the method [Stewart et al., 2010]. As the MTTs of this study are 5 and 10 years long, this makes an exact quantitative interpretation of the simulation result difficult at least. Furthermore, Kirchner [2016a] showed that a similar method to the convolution integral applied in this study, sine wave fitting to estimate MTT, is not able to reliably estimate MTTs. This so called aggregation bias error is caused by spatial heterogeneity and non-stationarities in the catchment [Kirchner, 2016a; Kirchner, 2016b]. As of yet, no similar investigation of the convolution integral exists, but the risk of the convolution integral suffering under the same aggregation bias must be considered. Thus, we deem the obtained TTDs and MTTs qualitatively, but not quantitatively, valid. This means that we consider the uncertainty connected with the exact shape of the TTD and the exact value of its MTT to be potentially very large, while the general conclusion of this study still holds true: higher resolution data influences estimates of TTD, emphasizing faster flow paths in the TTD. This is corroborated by our analysis of the fraction of young water in streamflow, which Kirchner [2016a] showed to be a reliable estimator, with weekly and high resolution data as discussed in the next section.

Overall, similar to findings of *Timbe et al.* [2015], this study found that the high resolution sampling scenario is preferable over the lower resolution one. Thus, when estimating TTDs, weekly isotope data can mislead our interpretation and concepts of internal catchment processes that govern water transport [*Hrachowitz et al.*, 2011]. Care must be taken regarding the temporal resolution when comparing the TTDs of different catchments to infer controls on the TTD (e.g., the isotope tracer studies of *Tetzlaff et al.* [2009a] and *Tetzlaff et al.* [2009b], comparing ten respectively 55 catchments). In cases where the temporal resolution of tracer data of the catchments in comparison does not match, TTD differences could be partly due to different temporal resolution of the used data [*Heidbüchel et al.*, 2012].

3.3 The fraction of young water estimated by sine wave fitting

According to *Kirchner* [2016a], we fitted sine waves to the precipitation and streamflow isotope data for weekly (Figure 9) and high resolution (Figure 10) data using iteratively reweighted least squares. The fitted cosine-coefficient for the high resolution and weekly precipitation data was determined with a large p-statistic (p = 0.44 and 0.92, respectively) and thus higher quantitative uncertainty, while the sine-coefficients and the constants for both data resolutions had considerably smaller uncertainties (p at least < 0.02, Table 4). For streamflow sine wave fitting, most parameters showed small p-statistics with the exception of the sine-coefficients for the weekly data resolution. We nonetheless used coefficients with large p-statistics in further calculations and assumed resulting errors to be small. As F_{yw} derived with the simple method gave very similar results when comparing it to results obtained with the more complex method (as discussed below), we could show that this assumption was justified. This was true for both data resolutions.

The calculated amplitudes and phase shifts lead to much more similar fitted sine waves in the case of precipitation than for streamflow when comparing both data resolutions. This indicates that the weekly bulk sample of precipitation water is sufficient to retain the seasonal pattern of the precipitation signal, with the seasonal variations in isotopes dominating the precipitation signal, while the weekly resolution grab samples of streamflow averaged-out unique information. This unique information could be isotopic peak events with a high weight, e.g., at the end of 2012 and the beginning of 2013 (Figure 10), which led to the twofold increase of the amplitude of high resolution streamflow data compared to weekly streamflow data (Table 4).

Using the simple method of deriving F_{yw} , where F_{yw} equals A_S/A_P , we found that the high resolution data revealed approximately a doubled amount of the fraction of young water when compared to the weekly resolution data (0.047 for weekly vs. 0.084 for high resolution, Table

5). Application of the more complex method led to very similar phase shifts between precipitation and streamflow for both data resolutions as well as similar shape factors of or the gamma-distributed TTD (weekly: $\varphi - \varphi = 50.36$ rad, $\alpha = 0.56$; high resolution: $\varphi - \varphi = 48.15$ rad, $\alpha = 0.54$). The scale factor β was markedly different with 320,960 for weekly data and 140,032 for the high resolution data case. Due to the similarity in of or both data resolutions, also the threshold age of young water τ_w was similar with 55 and 54 days for weekly and high resolution data, respectively (Table 5). For both data resolutions the calculated threshold age of young water is approximately the mean value of the wide uncertainty (weekly: 55 days with uncertainty of 47 to 67 days, high resolution: 54 days with uncertainty 49 to 60 days). Due to the strong similarity of the uncertainty for both data resolutions, it seems that the threshold age for young water is insensitive to the sampling frequency of tracer data.

Applying the complex method, F_{yw} was found to be 0.051 for weekly and 0.090 for high resolution data, comparing well to the simple method results of 0.047 and 0.084 (Table 5). These results define the tight uncertainty of F_{yw} . When propagating the uncertainty found during multiple linear regression to the results to obtain the wide uncertainty, the weekly data resolution varied with a fraction of young water from 0.038 to 0.070 being younger than 47 to 67 days. Results from the high resolution case varied with F_{yw} from 0.078 to 0.094 being younger than 49 to 60 days. Thus, the narrow uncertainty has approximately the same interval width for both data resolutions, while contrary to this the wider uncertainty is larger for the weekly resolution compared to the high resolution data set (0.038 to 0.070 versus 0.078 to 0.094, respectively). Thus, in the case of the fraction of young water (F_{yw}), the high sample resolution considerably reduced the uncertainty in F_{yw} .

The twofold increase in amplitude for the high resolution streamflow isotope data was responsible for the approximately twofold increase in the fraction of young water. The found

fractions of young water correspond well with recent findings of a global study of young water fractions conducted by *Jasechko et al.* [2016]. They found that a majority of the 254 investigated catchments had a fraction of young water between 0 and 30%, with an average of $26\% F_{yw}$.

Thus, in summary, when using weekly resolution data we found 4.7 - 5.1% of streamflow water being younger than 55 days, while when using high resolution data the results almost doubled to 8.4 - 9.0% being younger than 54 days.

Comparing the fraction of young water found at 55 (weekly) and 54 days (high resolution) to the corresponding cumulative TTD value at 55 and 54 days, we found a good agreement between estimating F_{yw} and inversely modeling TTD by means of the convolution integral (weekly: TTD value at 55 days of 0.039 compared to 0.051 F_{yw} , high resolution: TTD value at 54 days of 0.138 compared to 0.090 F_{yw}). Thus, although the convolution integral might be affected by aggregation bias error as suggested by *Kirchner* [2016a], at least in this study the estimates for faster flow paths derived from both methods are well comparable. Due to this, we recommend calculating the convolution integral TTD and the fraction of young water jointly in future studies to better investigate the relationship between those two measures under different catchment conditions.

4 Conclusion

In this study we investigated the influence of sampling frequency of tracer data on estimates of TTDs and the fraction of young water of a mesoscale catchment. For this purpose, we used sub-daily to daily and weekly stream and precipitation isotope tracer information. The stream isotope simulation results for both temporal resolutions captured the long-term dynamics well. The high frequency sampling data improved the simulation in terms of NSE, showing short-term dynamics that were not captured when using weekly data. This was reflected in the

respective TTDs, where the longer transit times of both data resolutions were similar and stronger deviations only occurred in the short transit time region. The use of daily to sub-daily tracer information also reduced the MTT by almost 50% compared to weekly data. When using high resolution data, the fraction of young water doubled compared to weekly data. Thus, both the convolution integral and the fraction of young water came to the same conclusion. Our results highlight the importance of sub-weekly isotope data on estimating TTDs or the fraction of young water and the associated risk of misinterpreting a catchment's water transport characteristics when using weekly measurements. Consequently, when comparing TTDs or young water fractions of different catchments, the temporal resolution of tracer data needs to be considered in the analysis.

Our study confirms that high resolution data is needed to be able to adequately characterize hydrological processes at the catchment scale [McDonnell and Beven, 2014], may they be reflected by the TTD or F_{yw} . Future research should focus on overcoming technical difficulties and establishing the high resolution isotope or chemical tracer data needed to ensure an improved understanding of catchment functioning [$Kirchner\ et\ al.$, 2004].

Acknowledgements

We gratefully acknowledge the support by the SFB-TR32 "Patterns in Soil-Vegetation-Atmosphere Systems: Monitoring, Modelling, and Data Assimilation" funded by the Deutsche Forschungsgemeinschaft (DFG) and TERENO (Terrestrial Environmental Observatories) funded by the Helmholtz-Gemeinschaft. Holger Wissel, Ulrike Langen, Werner Küpper, Rainer Harms, Phillip Meulendick and Ferdinand Engels are thanked for supporting the isotope analysis, sample collection and the ongoing maintenance of the experimental setup. We are grateful for the constructive suggestions of three anonymous reviewers and also acknowledge James Kirchner for helpful discussions about the young water fraction. The data used in this study can be acquired from the corresponding author.

References

Abbaspour, K. C., R. Schulin, and M. T. van Genuchten (2001), Estimating unsaturated soil hydraulic parameters using ant colony optimization, Adv Water Resour, 24(8), 827-841.

Berman, E. S. F., M. Gupta, C. Gabrielli, T. Garland, and J. J. McDonnell (2009), High-frequency field-deployable isotope analyzer for hydrological applications, Water Resour Res, 45.

Birkel, C., C. Soulsby, D. Tetzlaff, S. Dunn, and L. Spezia (2012), High-frequency storm event isotope sampling reveals time-variant transit time distributions and influence of diurnal cycles, Hydrol Process, 26(2), 308-316.

Bogena, H. R., M. Herbst, J. A. Huisman, U. Rosenbaum, A. Weuthen, and H. Vereecken (2010), Potential of Wireless Sensor Networks for Measuring Soil Water Content Variability, Vadose Zone J, 9(4), 1002-1013.

Bogena, H.R., R. Bol, N. Borchard, N. Brüggemann, B. Diekkrüger, C. Drüe, J. Groh, N. Gottselig, S.J. Huisman, A. Lücke, A. Missong, B. Neuwirth, T. Pütz, M. Schmidt, M. Stockinger, W. Tappe, L. Weihermüller, I. Wiekenkamp, and H. Vereecken (2015), A terrestrial observatory approach for the integrated investigation of the effects of deforestation on water, energy, and matter fluxes. Science China: Earth Sciences 58(1): 61-75, doi: 10.1007/s11430-014-4911-7.

Brand, W. A., T. B. Coplen, J. Vogl, M. Rosner, and T. Prohaska (2014), Assessment of international reference materials for isotope-ratio analysis (IUPAC Technical Report), Pure Appl Chem, 86(3), 425-467.

Brodersen, C., S. Pohl, M. Lindenlaub, C. Leibundgut, and K. von Wilpert (2000), Influence of vegetation structure on isotope content of throughfall and soil water, Hydrol Process, 14(8), 1439-1448.

Criss, R. E., and W. E. Winston (2008), Do Nash values have value? Discussion and alternate proposals, Hydrol Process, 22(14), 2723-2725.

Dewalle, D. R., and B. R. Swistock (1994), Differences in O-18 Content of Throughfall and Rainfall in Hardwood and Coniferous Forests, Hydrol Process, 8(1), 75-82.

Graf, A., H. R. Bogena, C. Drüe, H. Hardelauf, T. Pütz, G. Heinemann, and H. Vereecken (2014), Spatiotemporal relations between water budget components and soil water content in a forested tributary catchment, Water Resour Res, 50(6), 4837-4857.

Heidbüchel, I., P. A. Troch, S. W. Lyon, and M. Weiler (2012), The master transit time distribution of variable flow systems, Water Resour Res, 48.

Hrachowitz, M., C. Soulsby, D. Tetzlaff, J. J. C. Dawson, and I. A. Malcolm (2009), Regionalization of transit time estimates in montane catchments by integrating landscape controls, Water Resour Res, 45.

Hrachowitz, M., Soulsby, C., Tetzlaff, D. and Malcolm, I. A. (2011), Sensitivity of mean transit time estimates to model conditioning and data availability. Hydrol. Process., 25: 980–990. doi: 10.1002/hyp.7922.

Jakeman, A. J., and G. M. Hornberger (1993), How Much Complexity Is Warranted in a Rainfall-Runoff Model, Water Resour Res, 29(8), 2637-2649.

Jasechko, S., J. W. Kirchner, J. M. Welker, and J. J. McDonnell (2016), Substantial proportion of global streamflow less than three months old, Nat Geosci, 9(2), 126-129, doi:10.1038/ngeo2636.

Kato, H., Y. Onda, K. Nanko, T. Gomi, T. Yamanaka, and S. Kawaguchi (2013), Effect of canopy interception on spatial variability and isotopic composition of throughfall in Japanese cypress plantations, J Hydrol, 504, 1-11.

Kirchner, J. W., X. H. Feng, and C. Neal (2000), Fractal stream chemistry and its implications for contaminant transport in catchments, Nature, 403(6769), 524-527.

Kirchner, J. W., X. H. Feng, C. Neal, and A. J. Robson (2004), The fine structure of water-quality dynamics: the (high-frequency) wave of the future, Hydrol Process, 18(7), 1353-1359.

Kirchner, J. W. (2016a), Aggregation in environmental systems - Part 1: Seasonal tracer cycles quantify young water fractions, but not mean transit times, in spatially heterogeneous catchments, Hydrol Earth Syst Sc, 20(1), 279-297.

Kirchner, J. W. (2016b), Aggregation in environmental systems - Part 2: Catchment mean transit times and young water fractions under hydrologic nonstationarity, Hydrol Earth Syst Sc, 20(1), 299-328.

Klaus, J., K. P. Chun, K. J. McGuire, and J. J. McDonnell (2015), Temporal dynamics of catchment transit times from stable isotope data, Water Resour Res, 51(6), 4208-4223.

Kubota, T., Tsuboyama, Y., 2003. Intra- and inter-storm oxygen-18 and deuterium variations of rain, throughfall, and stemflow, and two-component hydrograph separation in a small forested catchment in Japan. J. Forest Res. 8 (3), 179–190.

McDonnell, J. J., and K. Beven (2014), Debates-The future of hydrological sciences: A (common) path forward? A call to action aimed at understanding velocities, celerities and residence time distributions of the headwater hydrograph, Water Resour Res, 50(6), 5342-5350.

Molenat, J., C. Gascuel-Odoux, L. Aquilina, and L. Ruiz (2013), Use of gaseous tracers (CFCs and SF6) and transit-time distribution spectrum to validate a shallow groundwater transport model, J Hydrol, 480, 1-9.

Nash, J. E., and J. V. Sutcliffe (1970), River flow forecasting through conceptual models: Part I - A discussion of principles, J Hydrol, 10(3), 282 - 290.

Rinaldo, A., K. J. Beven, E. Bertuzzo, L. Nicotina, J. Davies, A. Fiori, D. Russo, and G. Botter (2011), Catchment travel time distributions and water flow in soils, Water Resour Res, 47.

Roa-Garcia, M. C., and M. Weiler (2010), Integrated response and transit time distributions of watersheds by combining hydrograph separation and long-term transit time modeling, Hydrol Earth Syst Sc, 14(8), 1537-1549.

Rodgers, P., C. Soulsby, S. Waldron, and D. Tetzlaff (2005), Using stable isotope tracers to assess hydrological flow paths, residence times and landscape influences in a nested mesoscale catchment, Hydrol Earth Syst Sc, 9(3), 139-155.

Rosenbaum, U., H. R. Bogena, M. Herbst, J. A. Huisman, T. J. Peterson, A. Weuthen, A. W. Western, and H. Vereecken (2012), Seasonal and event dynamics of spatial soil moisture patterns at the small catchment scale, Water Resour Res, 48.

Stewart, M. K., Morgenstern, U. and McDonnell, J. J. (2010), Truncation of stream residence time: how the use of stable isotopes has skewed our concept of streamwater age and origin. Hydrol. Process., 24: 1646–1659. doi: 10.1002/hyp.7576.

Stockinger, M. P., H. R. Bogena, A. Lücke, B. Diekkrüger, M. Weiler, and H. Vereecken (2014), Seasonal soil moisture patterns: Controlling transit time distributions in a forested headwater catchment, Water Resour. Res., 50, 5270–5289, doi:10.1002/2013WR014815.

Stockinger, M. P., A. Lücke, J. J. McDonnell, B. Diekkrüger, H. Vereecken, and H. R. Bogena (2015), Interception effects on stable isotope driven streamwater transit time estimates, Geophys Res Lett, 42(13), 5299-5308.

Stoltidis, I., Krapp, L., 1980. Hydrological map NRW. 1:25.000, sheet 5404. State Agency for Water and Waste of North Rhine-Westfalia, Düsseldorf.

Tetzlaff, D., I. A. Malcolm, and C. Soulsby (2007), Influence of forestry, environmental change and climatic variability on the hydrology, hydrochemistry and residence times of upland catchments, J Hydrol, 346(3-4), 93-111.

Tetzlaff, D., J. Seibert, and C. Soulsby (2009a), Inter-catchment comparison to assess the influence of topography and soils on catchment transit times in a geomorphic province; the Cairngorm mountains, Scotland, Hydrol Process, 23(13), 1874-1886.

Tetzlaff, D., J. Seibert, K. J. McGuire, H. Laudon, D. A. Burn, S. M. Dunn, and C. Soulsby (2009b), How does landscape structure influence catchment transit time across different geomorphic provinces?, Hydrol Process, 23(6), 945-953.

Timbe, E., D. Windhorst, R. Celleri, L. Timbe, P. Crespo, H. G. Frede, J. Feyen, and L. Breuer (2015), Sampling frequency trade-offs in the assessment of mean transit times of tropical montane catchment waters under semi-steady-state conditions, Hydrol Earth Syst Sc, 19(3), 1153-1168.

Vereecken, H., J. A. Huisman, H. Bogena, J. Vanderborght, J. A. Vrugt, and J. W. Hopmans (2008), On the value of soil moisture measurements in vadose zone hydrology: A review, Water Resour Res, 44.

Viville, D., B. Ladouche, and T. Bariac (2006), Isotope hydrological study of mean transit time in the granitic Strengbach catchment (Vosges massif, France): application of the FlowPC model with modified input function, Hydrol Process, 20(8), 1737-1751.

Weiler, M., B. L. McGlynn, K. J. McGuire, and J. J. McDonnell (2003), How does rainfall become runoff? A combined tracer and runoff transfer function approach, Water Resour Res, 39(11).

Zacharias, S., H. R. Bogena, L. Samaniego, M. Mauder, R. Fuß, T. Pütz, M. Frenzel, M. Schwank, C. Baessler, K. Butterbach-Bahl, O. Bens, E. Borg, A. Brauer, P. Dietrich, I. Hajnsek, G. Helle, R. Kiese, H. Kunstmann, S. Klotz, J. C. Munch, H. Papen, E. Priesack, H. P. Schmid, R. Steinbrecher, U. Rosenbaum, G. Teutsch and H. Vereecken (2011), A Network of Terrestrial Environmental Observatories in Germany, Vadose Zone J, 10(3), 955-973.

Zimmermann, A., and B. Zimmermann (2014), Requirements for throughfall monitoring: The roles of temporal scale and canopy complexity, Agr Forest Meteorol, 189, 125-139.

Tables

Table 1. Percentage land use of the Erkensruhr catchment.

_	
Land Use	Fraction [%]
Grassland	36
Coniferous Forest	33
Deciduous Forest	22
Heath	3
Agriculture	2
Copse	2
Settlement	2

Table 2. Parameter values of the three modeling periods Winter_12, Summer_13 and Winter_13 for the hydrograph simulation (Sim), the event simulation (E) and the drying (D) and wetting-up (W) phase. Also shown are volumetric efficiency (VE) and the mean response time (MRT).

	Winter_12		Summer_13			Winter_13
	Sim	E	Sim	D	\mathbf{W}	Sim
b1 [-]	0.5	0.5	0.06	0.34	0.31	0.5
b2 [-]	10	10	1.14	5.18	5.42	10
b3 [-]	0	1	0.96	1	0.67	1
Tf [d]	5.5	5.4	12.0	11.7	23.0	4.9
Ts [d]	61.2	41.7	333.4	166.5	107.5	41.7
φ[-]	0.63	0.96	0.67	0.73	0.78	0.78
VE [-]	0.66	0.77	0.59	0.69	0.83	0.71
MRT [d]	26.1	6.8	118.1	53.5	41.6	13.0

b1, scaling parameter; b2, precipitation weighing parameter; b3, API at t = 0 (Equ. 2); Tf, fast reservoir mean residence time; Ts, slow reservoir mean residence time; ϕ fast reservoir contribution to RTD; VE, volumetric efficiency; MRT, mean response time.

Table 3. Parameter values of the high resolution and the weekly resolution TTD estimates. Also shown are the mean transit times (MTT) and the Nash-Sutcliffe efficiency values (NSE) when calculating the high resolution NSE only with weekly data points (weekly data) and with all data points (all), as well as the individual NSE for the phase before Winter_13 (before W_13) and for Winter_13 itself (W_13).

	High Resol	Weekly		
Tf [a]	0.55	0.56		
Ts [a]	9.89	10.64		
φ[-]	0.56	0.11		
NSE [-]	weekly data	all data		
	0.34	0.22	0.24	
	before W_13	W_13	0.24	
	0.34	-2.01		
MTT [a]	4.66	9.53		

Tf, fast reservoir mean residence time; Ts, slow reservoir mean residence time; \$\phi\$ fast reservoir contribution to TTD; NSE, Nash-Sutcliffe efficiency; MTT, mean transit time.

Table 4. Multiple linear regression coefficients (a, b) and constant (k) of the precipitation (subscript P) and streamflow (subscript S) sine wave fits and their respective p-statistic for weekly and high resolution data. Calculated from these values are the amplitude (A) and the phase shift (ϕ of each sine wave.

		High Resolution		Weekly	
		Value	p-statistic	Value	p-statistic
Precipitation	a_{P}	0.22	0.44	0.05	0.92
	b_P	-1.20	~ 0	-1.11	0.02
	k_{P}	-7.95	~ 0	-7.94	~ 0
	A_P [% o]	1.22		1.11	
P	φ [rad]	-0.18		-0.04	
Streamflow	$a_{\rm S}$	0.09	~ 0	0.04	0.08
	b_{S}	-0.05	~ 0	-0.03	0.27
	k_{S}	-8.58	~ 0	-8.54	~ 0
	A_S [% o]	0.10		0.05	
S	φ [rad]	-1.02		-0.92	

a, b, and k, regression coefficients and constant; A, amplitude; ϕ phase shift; subscripts P and S, precipitation and streamflow.

Table 5. Threshold age for young water (τ_{yw}) and fraction of young water (F_{yw}) results and the wide uncertainties for the weekly and high resolution data cases, respectively. Calculations were performed once with the simple (using only amplitudes) and once with the complex method (using the amplitudes and the phase shift). Comparison to TTD results is given under heading "TTD".

		Simple	Complex	TTD
W	τ _{yw} [days]	-	55	
	Uncertainty ^{a)}	47 - 67		0.039
	F_{vw}	0.047	0.051	0.0
	Uncertainty ^{a)}	0.038 - 0.070		
HR	τ _{yw} [days]	-	54	
	Uncertainty ^{a)}	49 - 60		0.138
	F_{vw}	0.084	0.090	0.1
	Uncertainty ^{a)}	0.078 - 0.094		

τ_{yw}, young water threshold; F_{yw}, fraction of young water; W, weekly resolution; HR, high resolution; TTD, cumulative TTD value at the threshold age.
a) Uncertainties only refer to the complex case error propagation

Figures

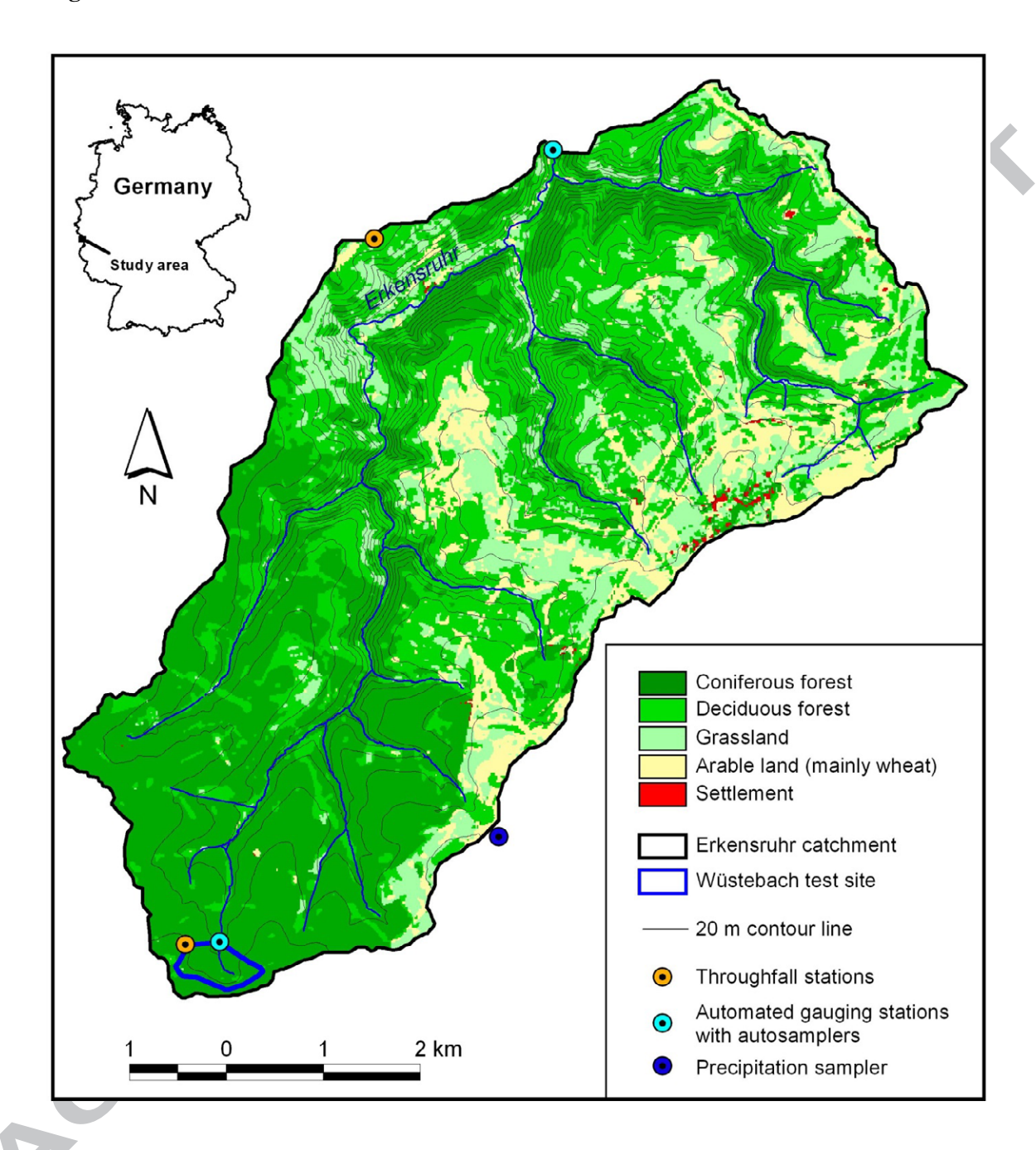


Figure 1. Location, elevation and land-use map of the Erkensruhr and the Wüstebach catchment.

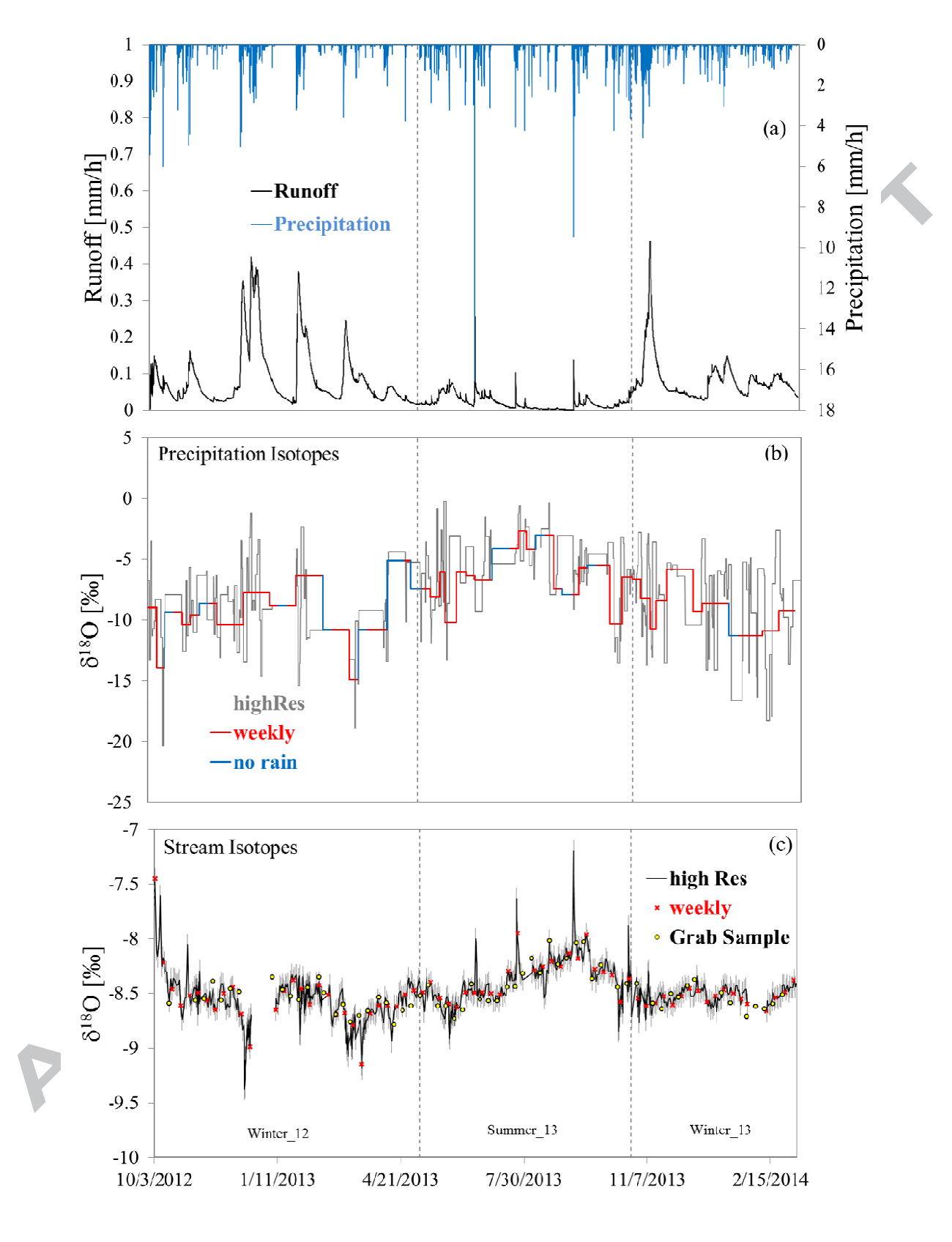


Figure 2. Measured and calculated data of the Erkensruhr catchment used for TTD estimation:

(a) runoff and precipitation, (b) precipitation isotopes with times when no rainfall was

recorded (no rain) and (c) stream isotopes with measurement error (grey, vertical lines engulfing the observed isotope time series). Isotopes were measured in high resolution (high Res) and calculated for weekly resolution (weekly), with manually taken stream samples for validation (Grab Sample, Panel c). The grey, vertical dashed lines in all panels delineate the three main modeling phases: Winter_12, Summer_13 and Winter_13.

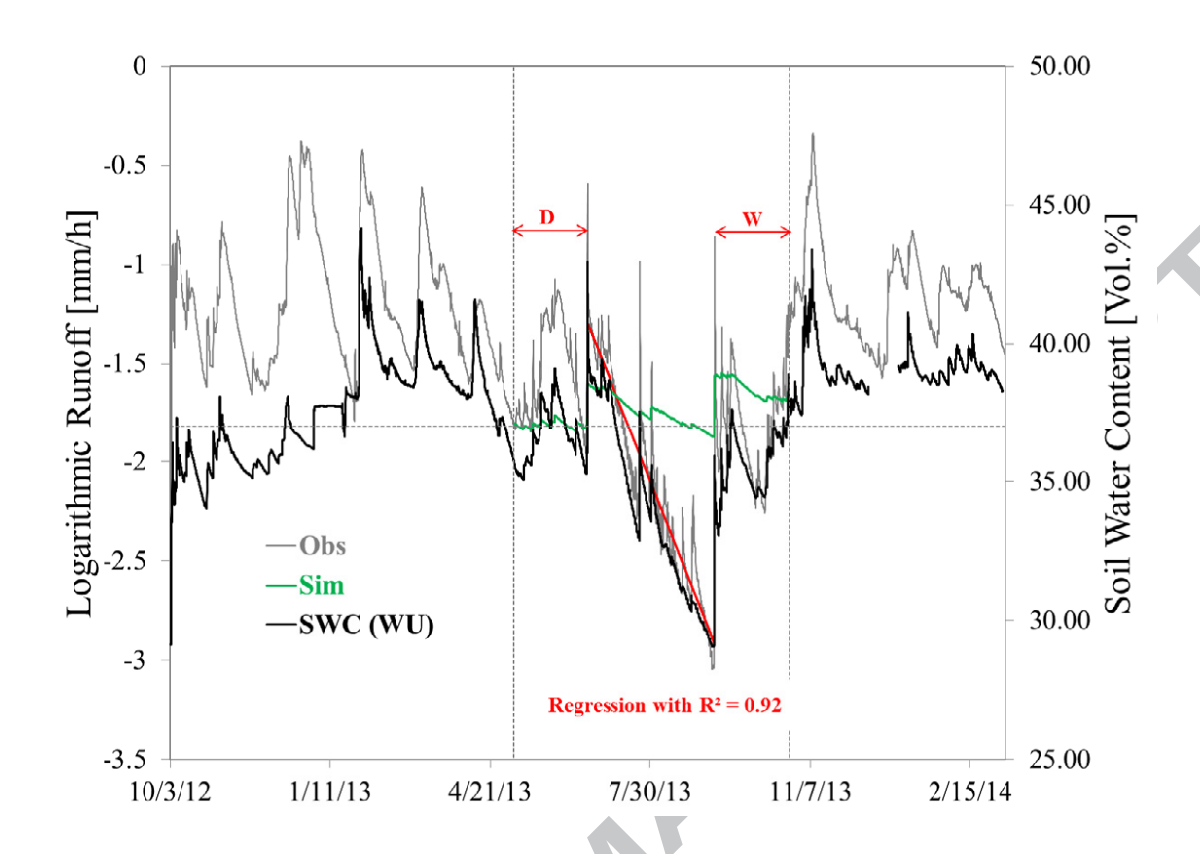


Figure 3. Logarithmic runoff (Obs) plotted with SWC measured at the sub-catchment Wüstebach (SWC (WU)). First simulation of Summer_13 resulted in an unrealistic solution (Sim). Thus, identifying a main phase using a linear trend with $R^2 = 0.92$ (red line), Summer_13 was split into this main phase, preceded by a drying (D) and followed by a wetting-up phase (W). Also shown is the separation of the complete time series into the three modeling periods (vertical, grey dashed lines) and the SWC limit for splitting the hydrograph (horizontal, grey dashed line).

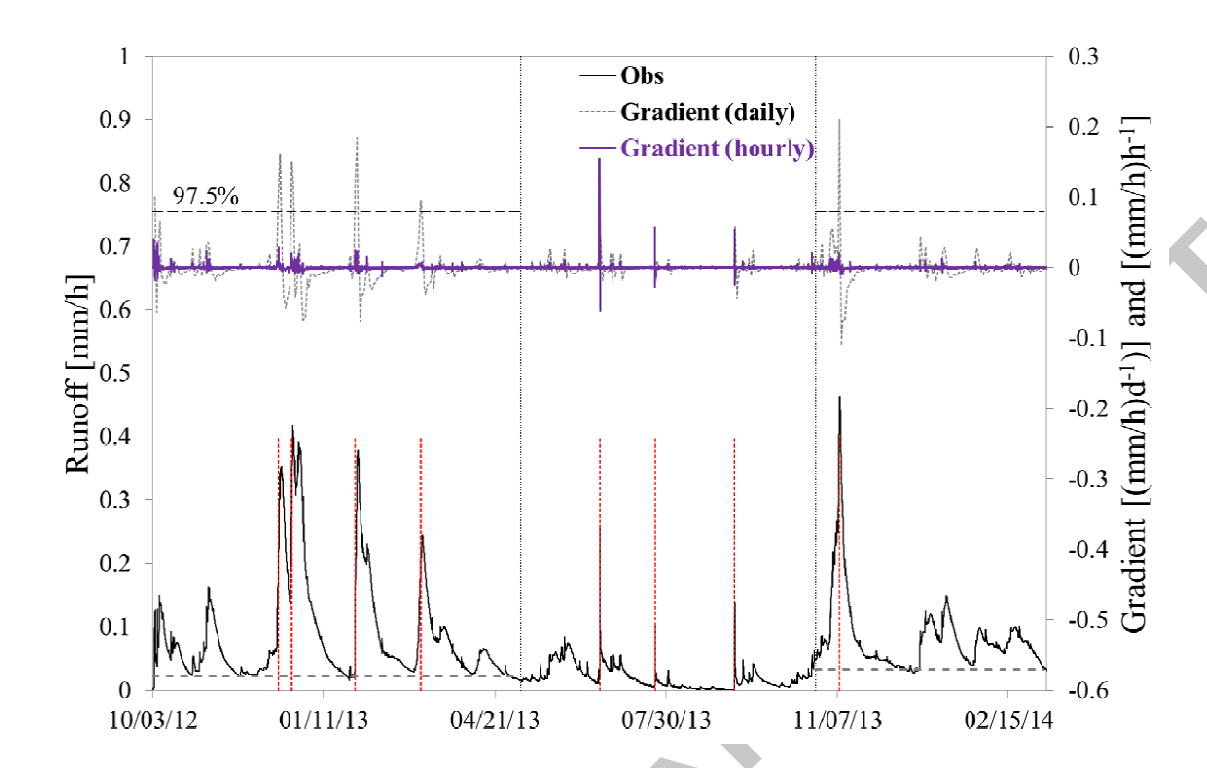


Figure 4. Identification of runoff events in the hydrograph (Obs) by using the 97.5% confidence interval of the daily hydrograph gradient (Gradient (daily)) and the 5%-quantile of runoff (horizontal, dashed grey lines) during the respective wet states. For the dry catchment state the hourly hydrograph gradient was used (Gradient (hourly)). Identified events are marked by dashed, red lines.

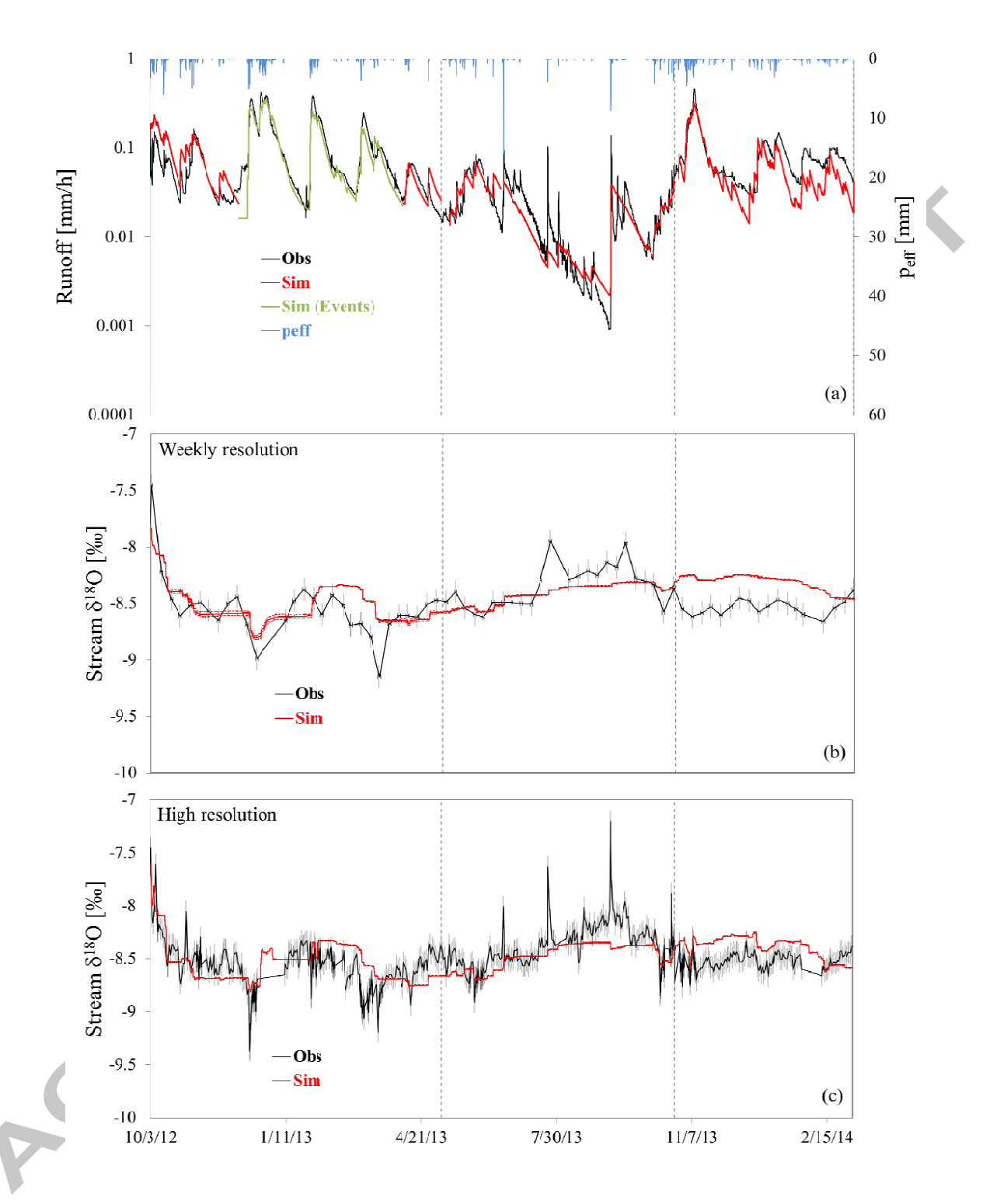


Figure 5. (a) Simulated runoff (Sim) with event modeling (Sim (Events)) plotted against observed runoff (Obs) on a logarithmic scale. Effective precipitation (p_{eff}) is shown as blue bars from the top; (b) and (c) Stream isotope modeling results (Sim) plotted together with observed stream isotopes (Obs) and their respective measurement uncertainties (grey lines)

using weekly and high temporal resolution. The narrow uncertainty of the simulation are shown as red dashed lines. Vertical, dashed grey lines in all panels denote the three modeling periods.



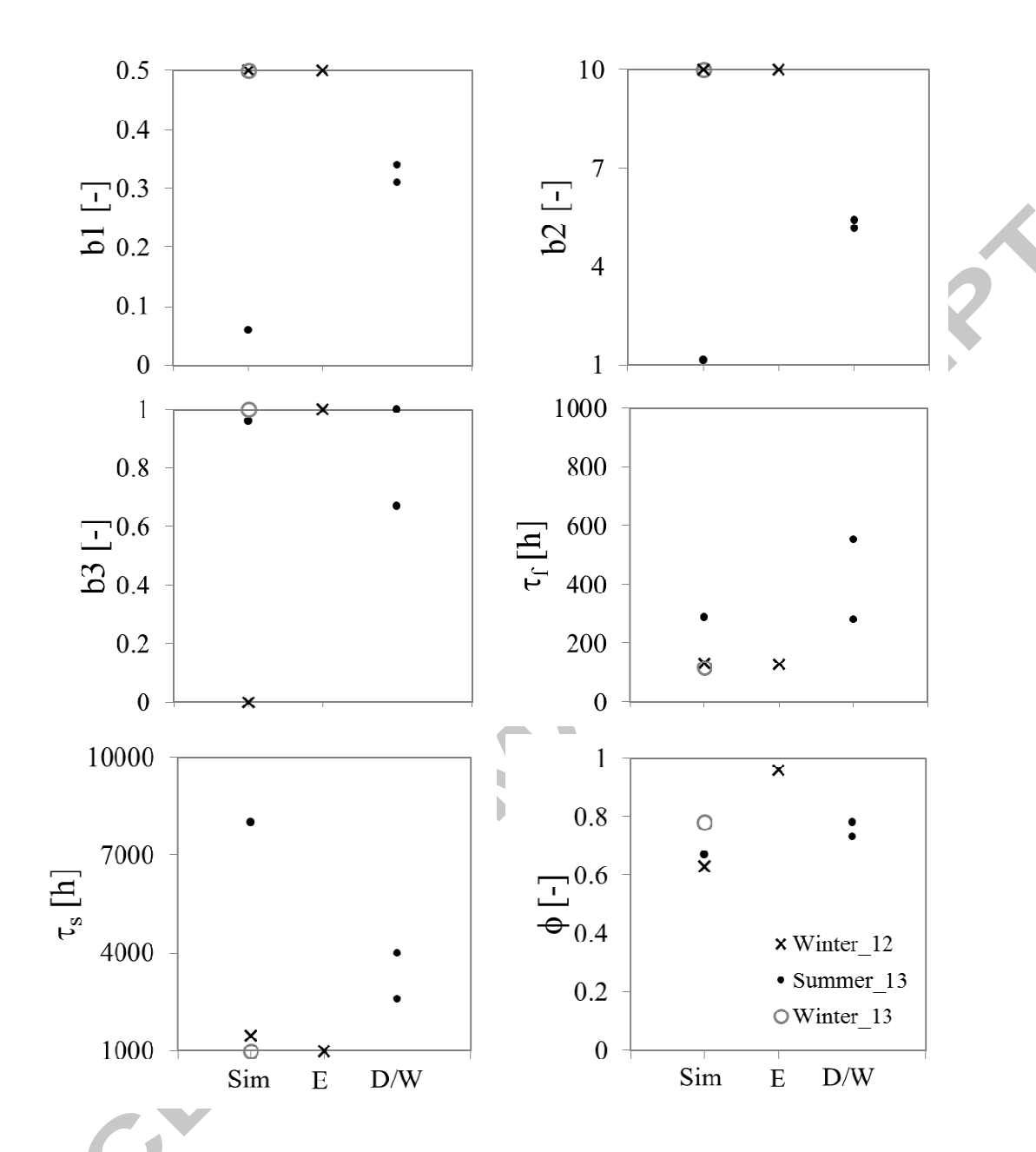


Figure 6. Parameter values of the hydrograph simulation with p_{eff} parameters b1, b2 and b3 and RTD parameters f, σ and ϕ displayed for the hydrograph simulation (Sim), the event case (E) and the drying and wetting phase (D/W). Vertical axis limits denote the parameter search boundaries.

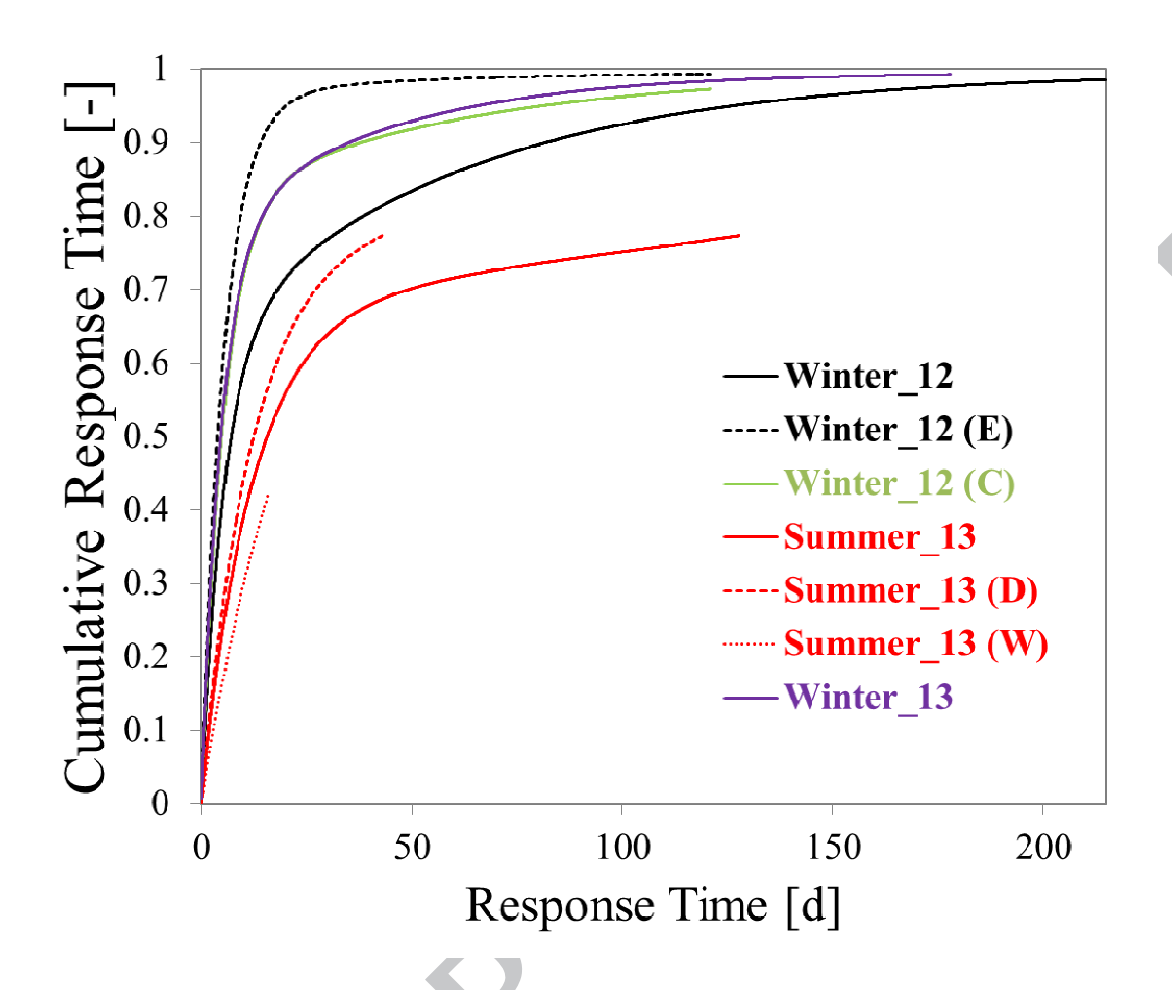


Figure 7. Response Time Distributions of the modeling phases: The three main modeling phases Winter_12, Summer_13 and Winter_13, as well as the event modeling (Winter_12 (E)). Summer_13 was sub-divided into a drying (Summer_13 (D)) and a wetting-up phase (Summer_13 (W)). The combination of the Winter_12 simulation with the event simulation Winter_12 (E), denoted as Winter_12 (C), resulted in a RTD comparable to Winter_13.

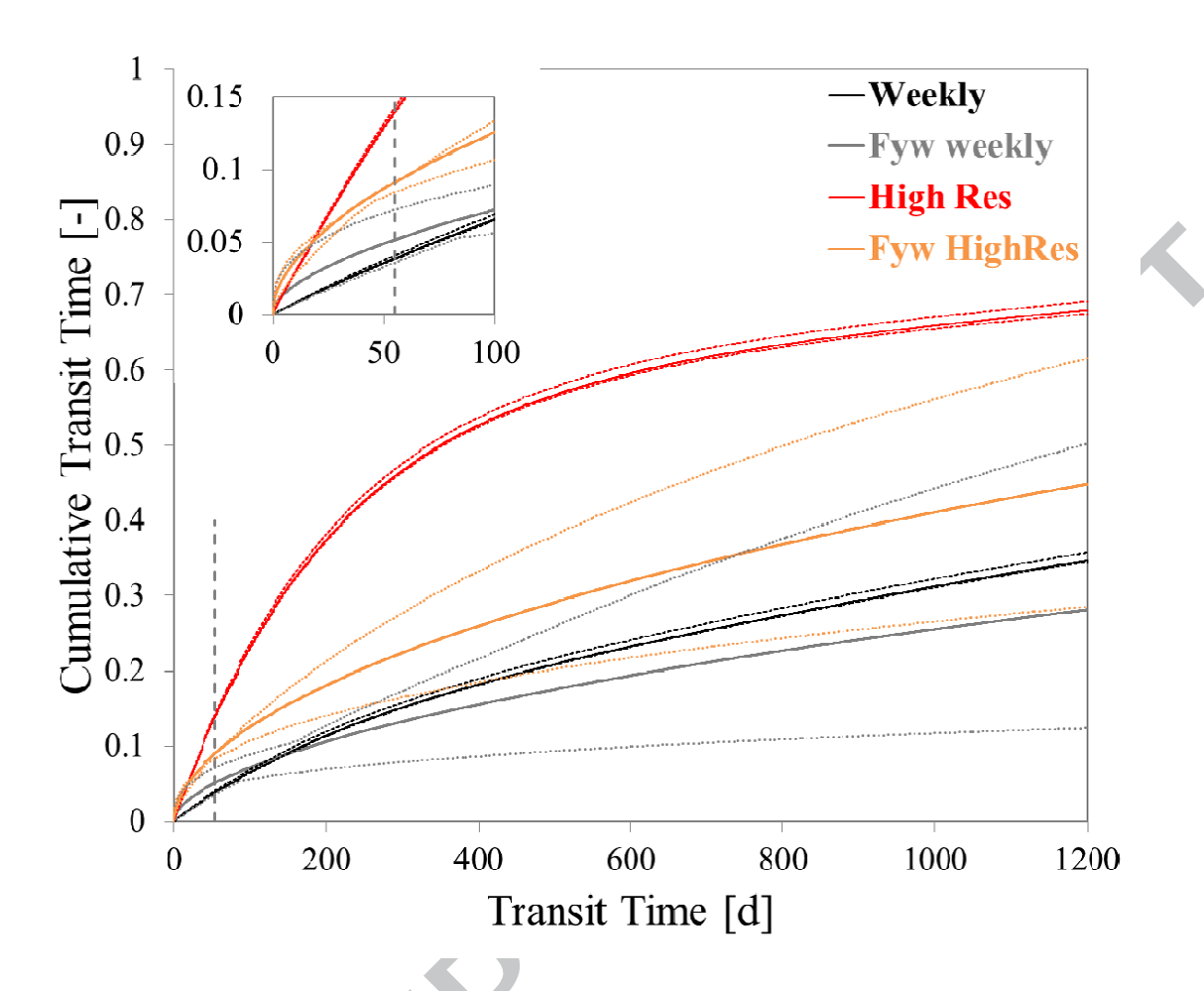


Figure 8. Transit Time Distributions based on weekly (Weekly) and high resolution (High Res) of precipitation and streamwater isotope data using the convolution integral. The gamma-distributed TTDs that were derived during the calculation of F_{yw} are displayed for weekly (Fyw weekly) and high resolution (Fyw HighRes) for comparison reasons. Uncertainty bands are shown as dashed lines, with the threshold age for young water shown as the vertical dashed line. Inset shows zoomed in details.

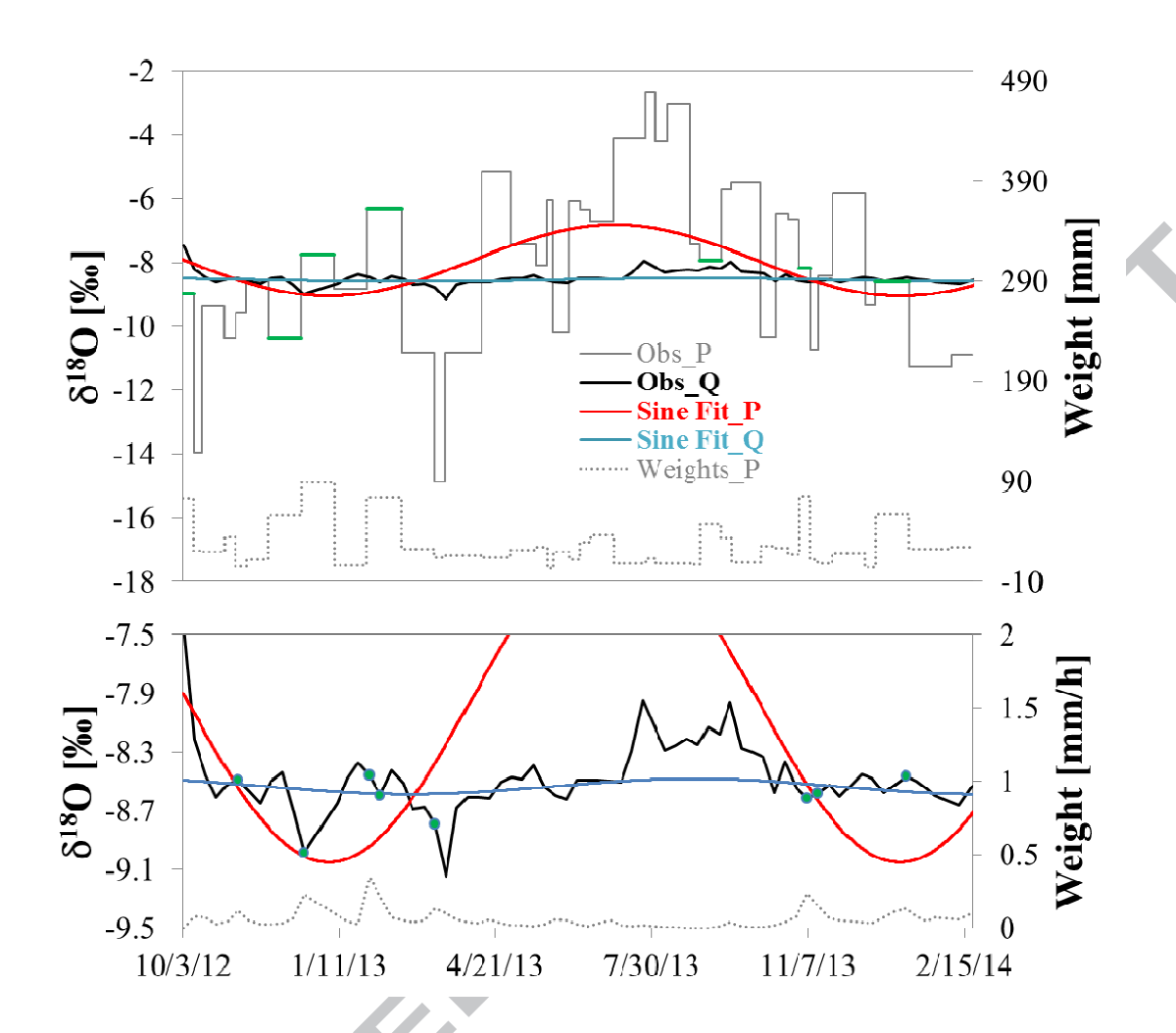


Figure 9. Sine wave fits (Sine Fit_P and Sine Fit_Q) of observed weekly precipitation and streamflow δ^8O isotope data (Obs_P and Obs_Q). The streamflow sine wave fit is shown in better detail in the lower panel. The applied weights are plotted as grey dotted lines in each panel and refer to precipitation weights in the top and streamflow weights in the lower panel. Weights that exceeded the mean plus the standard deviation are highlighted as green lines (top) or green dots (bottom).

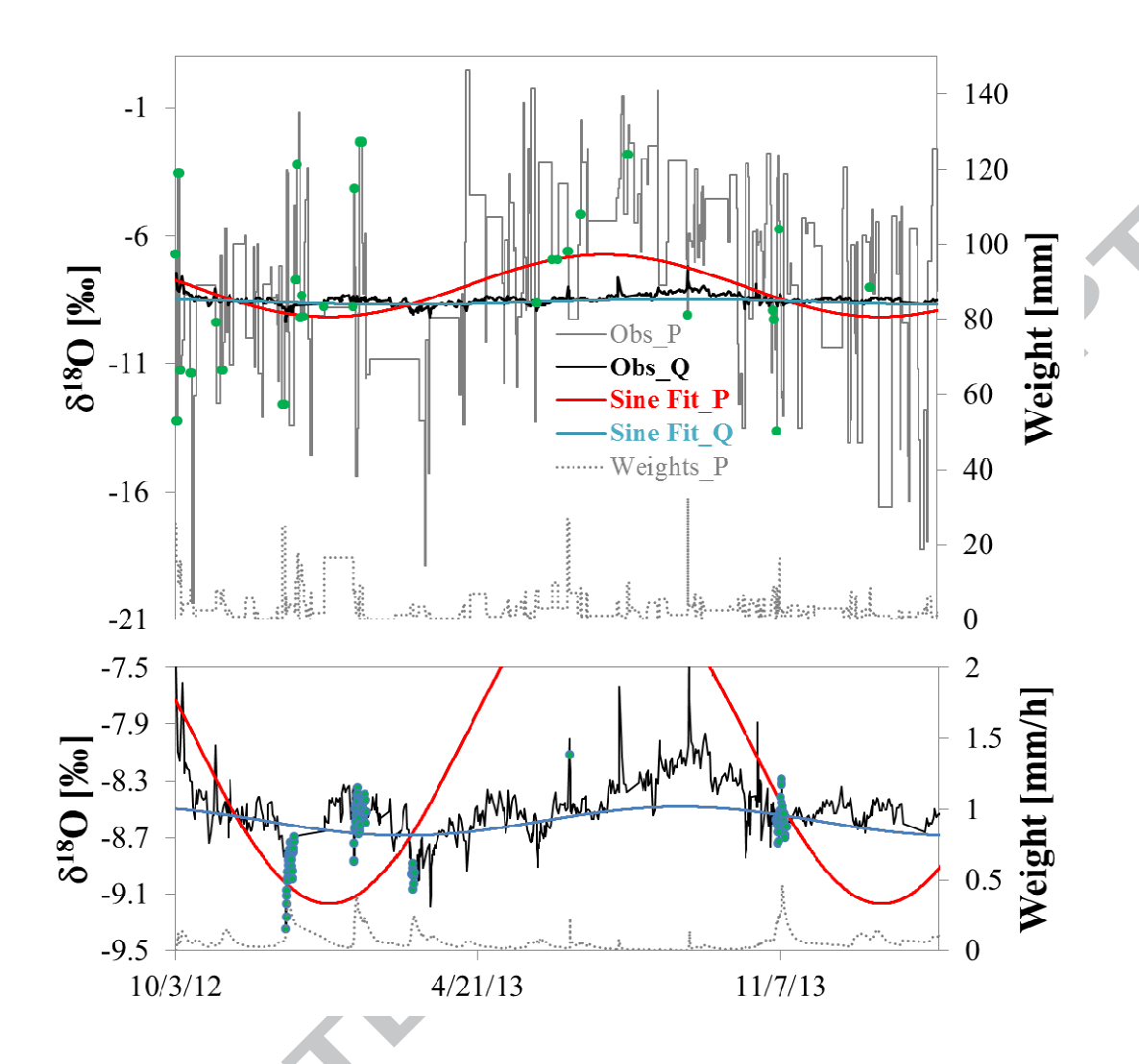


Figure 10. Sine wave fits (Sine Fit_P and Sine Fit_Q) of observed high resolution precipitation and streamflow δ^8 O isotope data (Obs_P and Obs_Q). The streamflow sine wave fit is shown in better detail in the lower panel. The applied weights are plotted as grey dotted lines in each panel and refer to precipitation weights in the top and streamflow weights in the lower panel. Weights that exceeded the mean plus the standard deviation are highlighted as green dots.

Highlights

- 1) The effect of sampling frequency on transit time distributions is explored
- 2) The effect of sampling frequency on the young water fraction is explored
- 3) Higher sampling frequency improves stable isotope tracer simulation results
- 4) Weekly sampling frequency lacks information of faster flow paths
- 5) Catchment comparison studies of transit time should consider sampling frequencies